Application of the ISPG Method in Various Manufacturing Processes Simulation

Li Zhang, Xiaofei Pan, Tung-Huan Su, Jingxiao Xu, C.T. Wu, Philip Ho

ANSYS, Inc.

1 Abstract

The Incompressible Smooth Particle Galerkin (ISPG) theory was proposed by the R&D team Computational and Multi-scale Mechanics Group (CMMG) at LSTC in 2017 [1]. It developed a new Incompressible Navier-Stokes solver to model free-surface Newtonian and Non-Newtonian fluid flow with surface tension and adhesion force. The Lagrangian particle method was employed to discretize the ISPG part to approximate the Navier-Stokes equation, coupled with surrounding rigid structures. The ISPG method is fully implicit, and in its dynamic mode, it simulates in real time fluid behaviors in many manufacturing processes. The ISPG's robust, in-core, and smart mesh adaptivity allows fluid flow in complex geometry, accurately capturing and aligning the ISPG surfaces with the structure surfaces while keeping the model size down. It also allows for separation and fusion within the ISPG fluid. The ISPG advanced material models allow for the simulation of fluid behavior with various viscosities from liquid to near solid state.

The ISPG technology was first applied in solder reflow simulation in 2019 [1]. Since then, with more features and improvements to the code, it has found itself in many other exciting areas of applications [2]. In this paper, we will summarize some of the basic ISPG capabilities, with a focus on showcasing the various applications of the ISPG method spanning many industries, including, but not limited to, compression molding, adhesive flow, and in the semiconductor manufacturing area, PCB (Printed Circuit Board) solder paste printing and stencil removal for soldering, capillary flow (underfilling) in the PCB/flip-chip packaging. The latter two are integral parts of the Chip manufacturing process. We will also discuss the limitations of the method in its current state.

2 Introduction/Background

The history of the ISPG method is relatively short. The first release of the method was made in LS-DYNA in 2019 (R12), where a semi-implicit version was used to calculate surface tension and adhesion force from solid structures. It is first applied in small-scale solder reflow simulation. Fully implicit versions of ISPG became available in 2020 (R13) and 2022 (R14), where both pressure and viscosity terms are solved fully implicitly. With the thermal feature, PCB package warping can be modelled in isothermal with heat transfer. The particle shifting technique was developed to guarantee an even distribution of particles. Solder reflows with 10K+ solder balls can now be simulated in multi-core MPP with a realistic solder mask, pad, PCB substrate, and die. Users' validation and feedback indicate the solder shapes can be predicted accurately.

Further enhancements in adaptive ISPG since 2022 have focused on in-core adaptivity, capabilities that align fluid surfaces with structure surfaces accurately with sharp edges and corners, and fluid part fusion and separation. Applications have started to develop in areas of adhesive flow, compression molding, thin-film coating, PCB board printing, PCB board adhesive capillary underfilling, and also potentially in gravity casting and giga casting.

The ISPG method, since it is a Lagrangian method, is easily accepted by users, especially for those users mostly working in the solid mechanics area. The method and its theories were described in detail in [1]. In this paper, we will focus on the aspects of usage, application and explain some basic capabilities of ISPG, followed by various application examples. Lastly, we will touch upon the advantages and limitations of the method in its current state.

3 Element

There are typically two types of components involved in an FSI type of simulation model: structure part and fluid part. In an ISPG model, the structure part must be modeled as solid elements, e.g. HEX, TETRA or PENTA with ELFORM of 1, 10, etc.; the fluid part (ISPG part) must be modeled as TETRA element with ELFORM=49. The ELFORM of 49 is a 3D type of ISPG formulation, which is automatically converted to the ISPG nodes (particles) for calculation.

4 Fluid Structure Interface (FSI)

The FSI contact is handled by the keyword ***CONTACT_ISPG_TO_SURFACE_COUPLING**. The SURFA side is always the fluid part, with either part ID or part set ID. The SURFB side is always the structure part, of which the surface segments that will likely come into contact with the fluid part are used for the definition. Here, one of the most important variables in FSI, the fluid/structure contact angle in static equilibrium, can be defined. The wall adhesion force is generated to maintain and satisfy this equilibrium contact angle. Fig.1 illustrates deformations of a water droplet in different contact angles θ, after dropping with its own gravity onto a rigid plate.

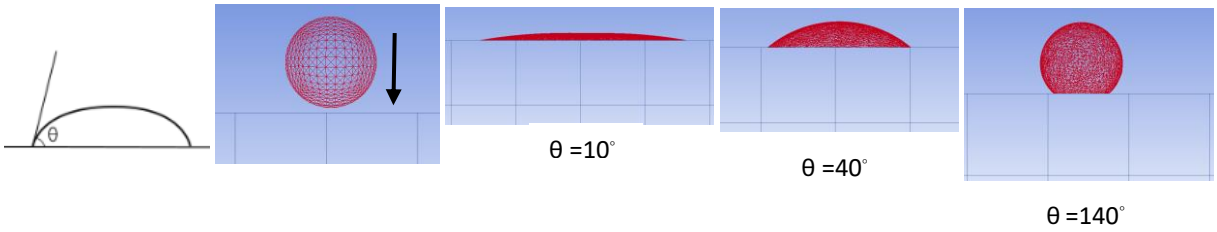

Fig.1: The deformations of a water droplet in different contact angles.

The contact angles (SCA), along with viscosity and surface tensions (defined in ISPG material models) for commonly used fluids/structures interactions are widely available on the web, although for a specific application, all variables need to be measured through experimental means.

The Wall adhesion force $\mathbf{F}_{\text{adhesion}}$ is applied on the contact edge of the ISPG fluid [3] and is pointed towards the structure interior. The contact angle is utilized to define the direction of the $\mathbf{F}_{\text{adhesion}}$, as seen in Fig.2. Depending on the velocity of the fluid contact edge for measurement of the contact angles, $\mathbf{V}_{\text{edge}}$ either points away from the fluid or towards the fluid.

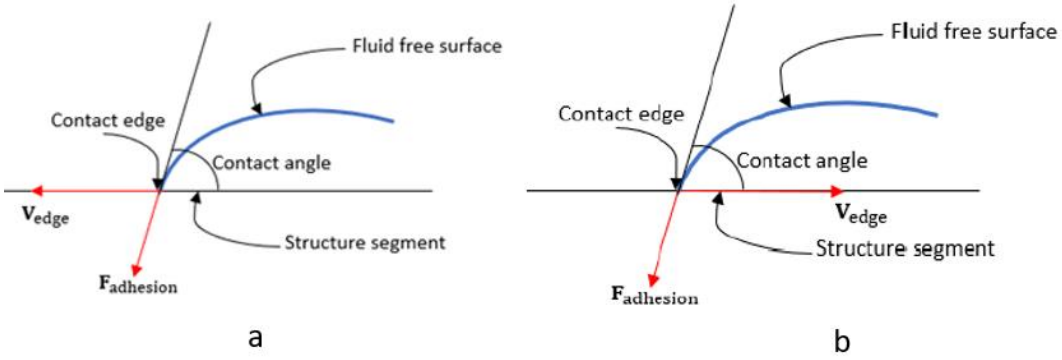

Fig.2: Contact between ISPG and structural segments.

The boundary condition (SBC) for contact edges can also be defined here. The fluid contact edges can be defined to move on the structure surface, tie with the structure surface (non-slip) or in a free-slip condition. A setting of SBC=0 usually applies in cases such as solder reflow, capillary driven underfilling flow, adhesion dominant applications. A setting of SBC=1 would be used in cases where viscosity is high, such as compression molding of semi-solid liquid metal. A value of SBC=2 is used for lower viscosity fluid, such as water, gravity casting, etc. Incorrected SBC setting could result in unexpected behaviors.

A very useful, new variable THK can be defined in cases where a shell structure part is offset in thickness direction to create a solid structure. Oftentimes it is difficult to make the resulting solid structure part large enough of a thickness required by ISPG contact, so this variable THK can be set to a bigger value than the actual solid structure thickness which will satisfy the contact stability requirements.

5 Adaptive Remeshing

The element formulation 49 automatically utilizes the adaptivity technique to guarantee even distribution of particles. The adaptivity procedure for the ISPG is as following, referring to Fig.3,

1. Nodes insertion and deletion operations are deployed based on the algorithm described in [4].
2. Nodes-cloud based remeshing is used, and convex meshing is always generated.

3. A Surface-cleaning technique is developed to remove the redundant elements and recover the geometry.

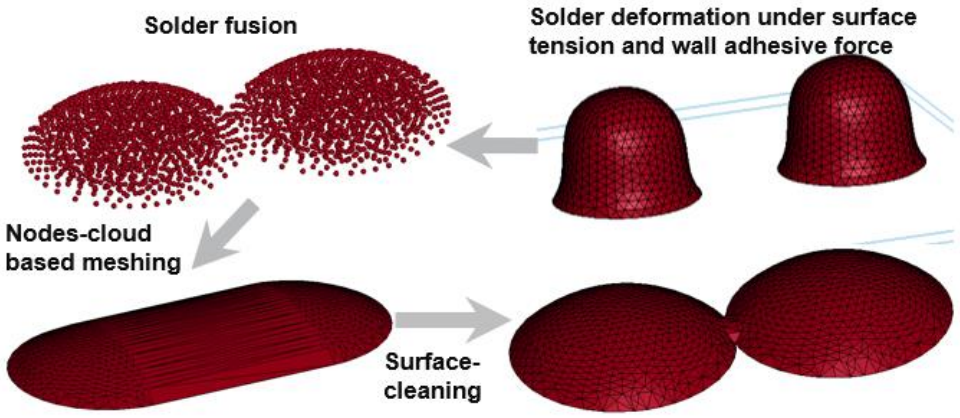

Fig.3: Nodes-cloud based remeshing technique for the adaptive ISPG.

Adaptive remeshing in ISPG fluid is very easy to use in part due to its advanced and highly efficient remeshing algorithm. The fluid remeshing can capture and align exactly with the structure shapes. Unlike in 3D adaptive remeshing in solid mechanics, the structure mesh is not required to have a fillet, radius, etc. The refined mesh is also very efficient, meaning regions/areas immediately outside the direct contact with the structure get coarsened mesh in a sharp gradient. There are also no inputs required for the min/max element size, the adaptive frequency/intervals, etc. to specify as in solid mechanics. Here we will touch upon a few variables users most likely need to consider.

ALIGN: Control the alignment of fluid nodes with the structure nodes, based on the critical angle of adjacent structure segments. Setting this value to “1“ allows the code to automatically align, resulting in a perfect alignment. Setting this value to “2“ allows for a faster turnaround time, while maintaining a reasonable fluid/structure mesh alignment.

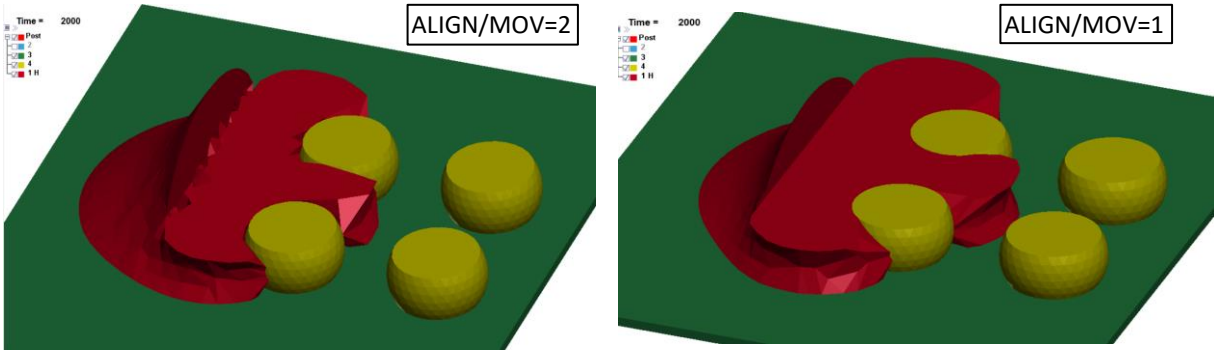

Fig.4: The effect of ALIGN and MOVE in a flip-chip underfilling simulation.

MOVE: Staggering algorithm [3] for fluid free edge move. This is developed for cases where structure segments are discontinuous (sharp corners and edge), like in many models from the semi-conductor industry. In fact, most models tend not to have any radii and fillets. Setting this value to “2” allows for faster computation time. Fig.4 shows the effect of different settings of ALIGN and MOVE in a flip-chip underfilling process simulation. With ALIGN/MOVE set to “2”, the fluid meshes do not fully match the solder ball shapes when compared to ALIGN/MOVE=1; also, the fluid front moves slower than that of ALIGN/MOVE=1 and its shape is different. The effect on the computation time can be dramatic, especially for large models.

OPT: This variable is the number of quadrature points used for the fluid elements to detect the boundaries of the structure ones. Only one quadrature point will be used to detect the penetration if OPT=0; this applies in cases such as solder reflow, underfilling application, etc. For OPT=1, five quadrature points will be used, and more strict detection is conducted; this is used in cases of some complex tool geometries where thickness is very thin, in compression molding and in pressurized casting (gigacasting) simulation.

6 Material Model

There are many material models available for the ISPG fluid [3]; two of which are discussed here.
The Newtonian fluid properties are defined with ***ISPG_MAT_ISO_NEWTONIAN**, where surface tension, fluid density and viscosity can be specified.
The keyword ***ISPG_MAT_CARREAU** can be used to cover a wide range of fluids with curve-fitting to piece together both Newtonian, shear thinning (n<1) and shear thickening (n>1) non-Newtonian fluids. The Carreau model's viscosity η is described as [3],

$$\eta(\dot{\gamma}) = \eta_\infty + (\eta_0 - \eta_\infty)(1 + \dot{\gamma}^2\lambda^2)^{\frac{(n-1)}{2}}$$

where the shear rate $\dot{\gamma} = \sqrt{\frac{1}{2}\bar{\bar{D}}:\bar{\bar{D}}}$ is computed based on the second invariant of the rate-of-deformation tensor $\bar{\bar{D}} = \left(\frac{\partial v_j}{\partial x_i} + \frac{\partial v_i}{\partial xj}\right)$, η_0 and η_∞ are viscosities at zero- and infinite-shear rate, respectively, λ is a time constant, n is the power law index. Typical variations of viscosity with shear rate according to different shear thinning non-Newtonian fluids is illustrated in Fig 5a. The material constants are experimentally determined with curve fitting. An example of a curve fitting using the Carreau model is shown in Fig.5b.
The typical unit systems used are kg, kN, mm, ms, GPa, GPa*ms; and, g, N, mm, ms, MPa, MPa*ms. The selection of the unit system is important for a successful simulation. A rule of thumb is to avoid very small decimal values causing round-off errors.

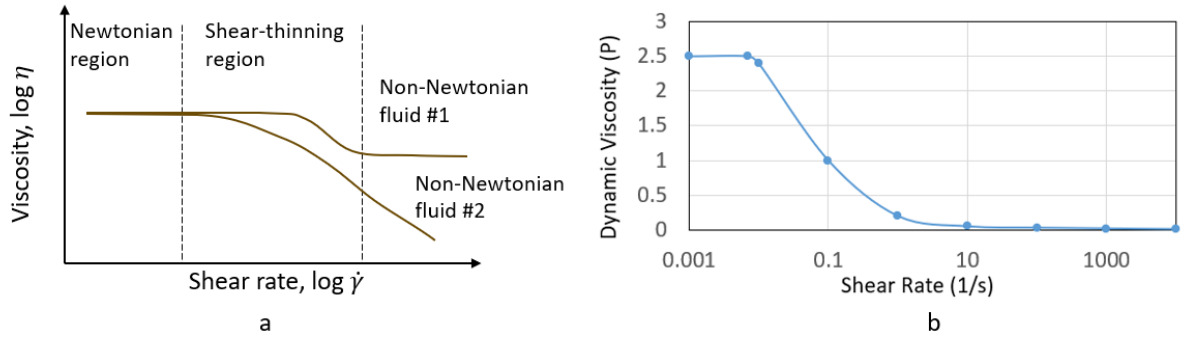

Fig.5: **a** *Viscosity with shear rate dependence.* **b** *An example of the Carreau model.*

In many industrial applications, temperature plays an important role in the properties of materials. Temperature dependence along with the shear rate dependence need to be considered for viscosity models. When the temperature is involved, the total viscosity μ in ISPG is calculated as:

$$\mu = \mathrm{H}(T)\eta(\dot{\gamma})$$

where $\eta(\dot{\gamma})$ is the shear rate dependence and $\mathrm{H}(T)$ is the temperature dependence, known as the Arrhenius law,

$$\mathrm{H}(T) = \exp\left[\alpha\left(\frac{1}{T - T_0} - \frac{1}{T_\alpha - T_0}\right)\right]$$

where α is the ratio of the activation energy to the thermodynamic constant and T_α is the reference temperature (default=273.15 Kevin), T_0 is the temperature shift (default=0.0). If the parameter α is set to 0, the temperature dependence will be ignored due to $\mathrm{H}(T) = 1$ and only the shear rate dependence term $\eta(\dot{\gamma})$ will be considered in the ISPG solution procedure. In the latest development version, ***ISPG_CONTROL_SOLUTION** is used to activate the thermal-flow analysis solution.
The ISPG thermal-fluid flow analysis requires thermal properties (i.e., specific heat and thermal conductivity coefficient) of the ISPG part to be defined with ***ISPG_MAT_THERMAL**. For the thermal boundary condition of the ISPG fluid parts and the environment (i.e., convective boundary condition at the free surface of the ISPG parts), surface heat flux across the free surface is described by the heat convection coefficient (HTC) at the boundary, pointing in the direction of the boundary normal of ISPG parts, and the environment temperature. The HTC and the environment temperature are defined with ***ISPG_BOUNDARY_CONVECTION_SET**. Similarly, the latest development version enables one-way thermal contact between fluids and structure parts. HTC for thermal boundary condition between the ISPG nodes and the structural surface can be defined with ***DEFINE_ISPG_TO_SURFACE_COUPLING**. The Initial temperatures of the structure parts are defined in ***INITIAL_TEMPERATURE_SET** and is

automatically retrieved in the ISPG thermal-flow analysis procedure, while the initial temperatures for the ISPG part are defined with ***ISPG_INITIAL_TEMPERATURE_SET**.

7 Implicit Dynamics

The ISPG method is an implicit dynamic method, therefore must be run in double precision. Before starting to run an ISPG simulation, if the structure parts are not stationary, a dynamic implicit simulation on the structure parts alone (all the usual implicit cards apply) should be performed first to ensure the contact and various implicit settings (DT0, DTMAX, etc.) are optimal and efficient, and simulation behaves correctly, and convergence is achieved; this is especially important if the structure involves deformable parts. For an ISPG simulation, if all structures involved are rigid bodies that move, DT0 should be adjusted according to the ISPG convergence rate for an efficient simulation. Implicit controls for the ISPG are provided by ***ISPG_CONTROL_IMPLICIT**. The ISPG convergence criteria include relative and absolute norms for velocity, pressure, and temperature terms. The relative tolerance for velocity/pressure/temperature is 1.0E-4, and the absolute tolerances for velocity, pressure, and temperature are 1.0E-12, 1.0E-16, and 1.0E-12, respectively. The two most used variables are MX_SUBS (maximum ISPG sub-cycles in each structure time step), and MX_ITERS (maximum ISPG iteration numbers in each sub-step). The structural and ISPG implicit cycles go as follows,

1. Iterations on structure are performed per current step size, step size cutback will be performed per structure implicit auto-stepping if so specified. For structures comprised of only rigid bodies, this step is very easy to converge.
2. The critical time step size for ISPG is determined by the CFL condition, which leads to the number of sub-cycles.
3. ISPG sub-cycling begins. Once the convergence criteria for the current sub-cycle are met within the specified maximum ISPG Newton-Raphson iterations (MX_ITERS), it moves onto the next sub-cycle until all sub-cycles are completed.
4. If ISPG iterations do not converge within each sub-cycle (fluid velocity is too fast), additional sub-cycles are generated until convergence is achieved. Likewise, the sub-cycle number will automatically reduce if convergence is achieved (fluid velocity is too slow).
5. If MX_SUBS (default: 512) is reached, the ISPG time step will not drop anymore, therefore no more sub-cycling. This is an indication that the simulation is going unstable; the model or variable settings including the ISPG material property inputs may need to be examined.
6. Otherwise, the next structural implicit step begins, with the ISPG sub-cycles to follow, so on and so forth.

In LS-DYNA R16, the ISPG method runs in MPP with multiple cores on a solder reflow process simulation and runs in one core for other applications.

8 Application Examples

8.1 Water

These examples show the behaviors of water as they are easily related to. In Fig.6, an initially spherical water droplet (density: 1.0E-3 g/mm^3; viscosity: 1.0E-6 MPa*ms; surface tension: 7.28E-7 N/mm; contact angle: 0.698 radian) is dropped and squashed between two rigid plates to a gap of 0.05mm. Figs.6a, 6b show its initial and after gravity dropped shapes on a side view; Fig.6c shows the droplet in its final flattened configuration on a top view. A smaller gap (<0.05mm) is also possible.

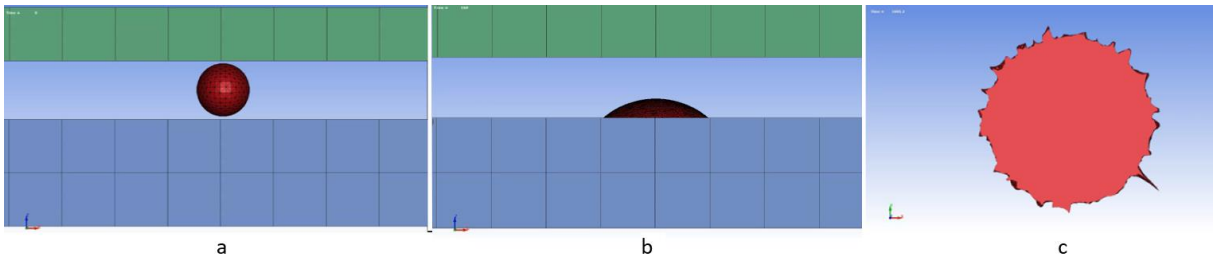

Fig.6: A water droplet dropped and squashed between two rigid plates to a thickness of 0.05mm.

In Fig.7, a long bead of water is dropped onto an edge formed by two rigid plates, underfills the gap of 0.2mm formed by the plates and emerges underneath the overhang area of the top plate, and completely detached from the lower plate. Figs.7a, 7b show the initial configuration viewed from side and top,

respectively. Figs.7c, 7d show an intermediate and the final shape from the top view, respectively; Fig.7e shows the water bead in its final configuration on a side view, which now takes the shape of an upside-down sphere cap.

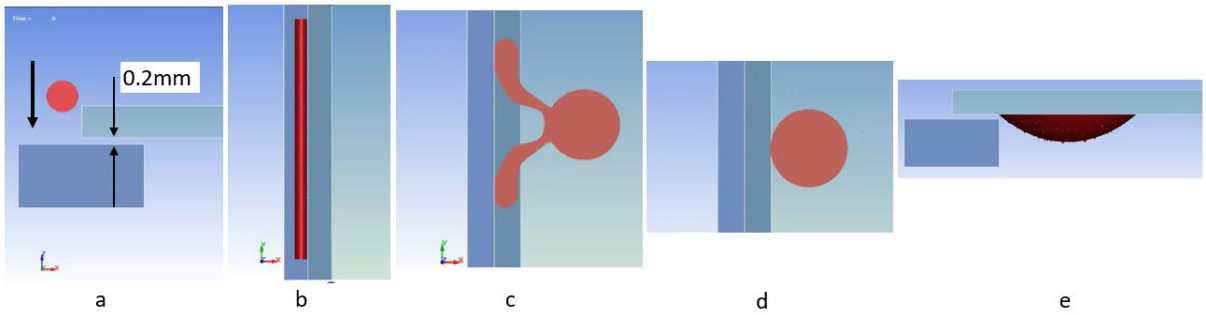

Fig.7: A long water bead dropped and underfills a gap of 0.2mm between two plates.

8.2 Metal

Liquid and semi-liquid metals are used in casting, consumer electronics, medical components, interconnects, etc. In Fig.8a, a column of steel with a square cross-section is being dropped onto an inclined plate on the left that bends into a horizontal plate on the right. Viscosities vary from 1.9E-7, 7.0E-5, 3.9E-5, 7.0E-4, 7.0E-3, and1.9E-2 GPa*ms, corresponding to the results shown in Figs. 8b, 8c, 8d, 8e, 8f and 8g, respectively. As expected, at a very low viscosity (Fig.8b) the metal behaves more like water. At the highest viscosity (Fig.8g), the metal behaves almost like solid metal; it slides down the ramp after contact, with the top portion eventally resting on the upstanding flanging. It is interesting to see as the viscosity increases, the square cross-section and the vertical column edges becomes more visible from the final resting shapes (Figs.8c~8f). The ISPG contact coupling with the plate worked very well.

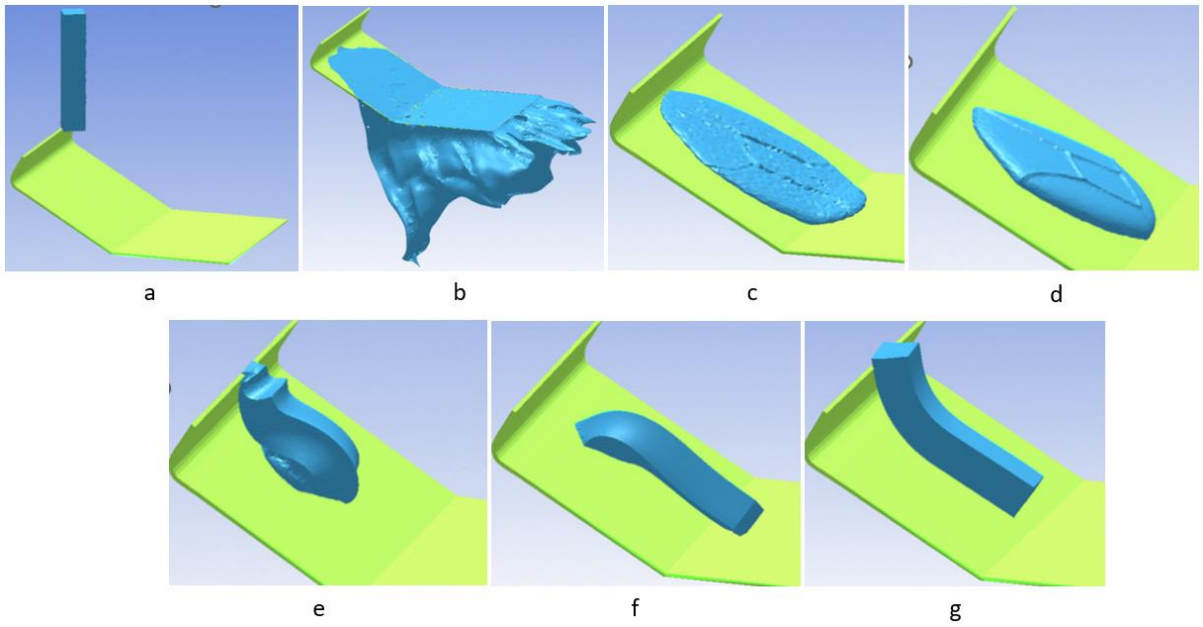

Fig.8: A square column of metal (a) dropping onto a plate, from (b) to (g) with increased viscosities.

In Fig.9, an elliptical shaped semi-liquid metal body (density: 2.7E-3 g/mm^3; viscosity: 3.0E-5 MPa*ms; surface tension: 2.0E-5 N/mm; contact angle: 0.698 radian) is dropped first with gravity onto a cavity mold at t=0. At t=275ms, the semi-liquid metal settles down under gravity; then the upper die comes down to form the liquid metal into the mold with narrow channels (0.05mm gap) around the mold's perimeters for the metal to escape as flashings, finishing up at t=380ms. Although sharp corners and edges are everywhere on the structure parts, the ISPG mesh adaptivity and fluid and structure coupling maintained perfect contact conditions. At t=380ms, we can even see the liquid metal overflowing the top edge of the cavity mold. Total simulation time including gravity took about 5 hours on one core MPP. In

Fig.10, the cross-sectional fringe contours of a thermal flow simulaiton in the same mold are shown. The initial fluid temperature is set at 843K, mold temperature at 423K, and the ambient temperature at 298K. Temperatures of the fluid are shown at t=0, t=180ms (gravity) and t=384ms (mold fully closed). At t=180ms (Fig.10b), The ISPG surface temperatures in contact with the mold surfaces have lower temperatures than those in the middle of the fluid. At completion (Fig.10c), the entire fluid body cooled down substantially, with a reduced temperature gradient. Initial viscosity in the ISPG part is shown in Fig.10d, which is consistent with the input. The final viscosities shown in Fig.10e vary based on the temperature distribution in the fluid. Lower temperatures result in higher viscosities and vice versa. In fact, the metal portions (which ran up the long flashing channel and exposed to air) that overflowed the flashing opening showed less fluid like behavior because of the lower viscosity levels.

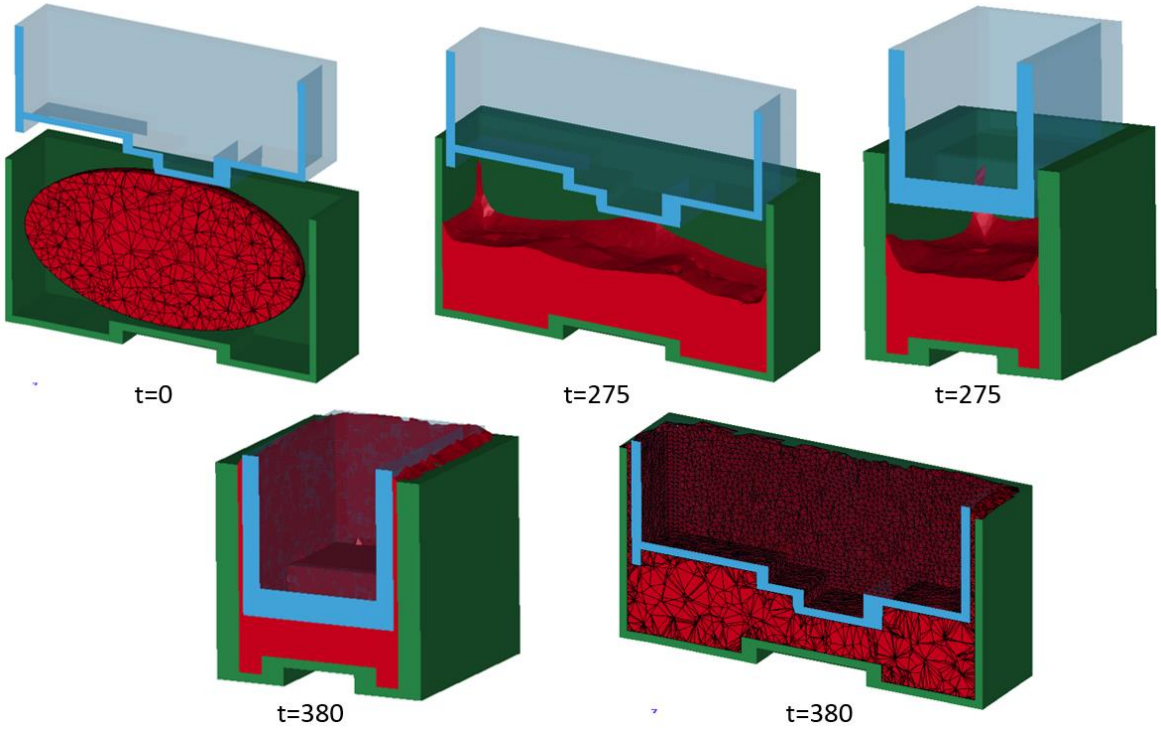

Fig.9: Gravity pouring and compression molding (time unit: ms).

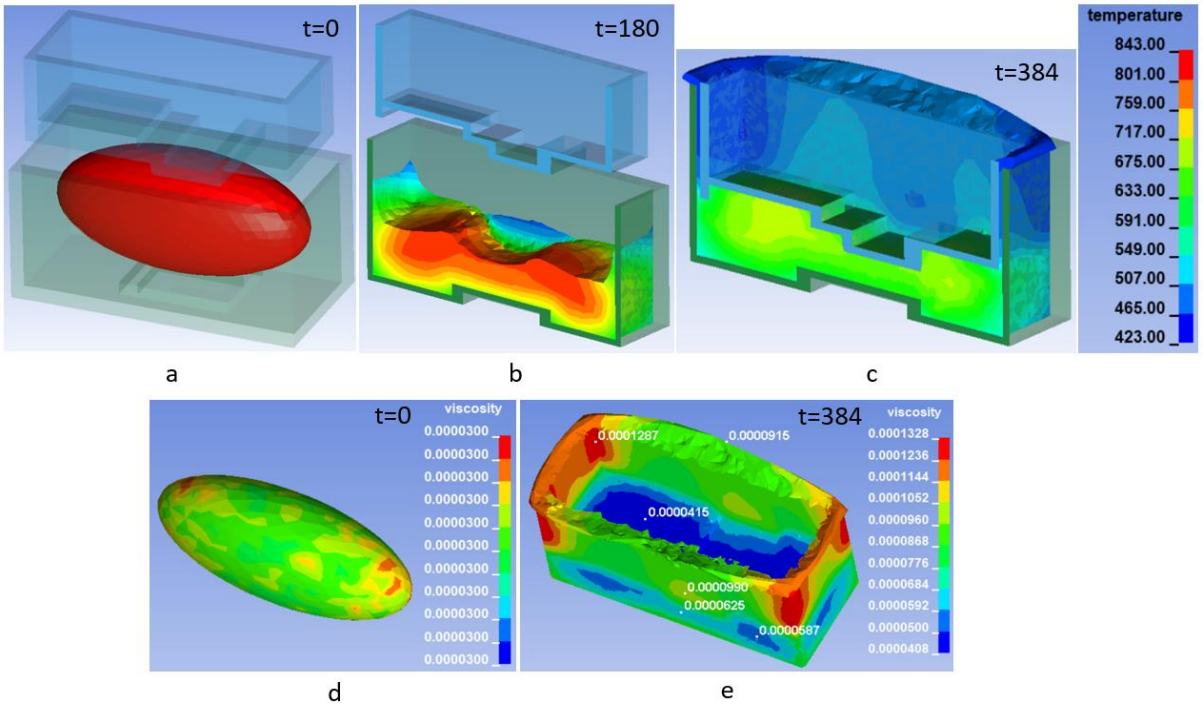

*Fig.10: Thermal flow simulation of gravity pouring and compression molding (unit: ms, Kelvin, MPa*ms)*

8.3 Adhesive

Adhesives are widely used for bonding materials in various industries, such as automotive, electronics, medical, optical, chemical, and oil and gas industries, to bond a range of metals, ceramics, glass, plastics, rubbers and composites, etc. The filling process, the fillibility into tight gaps and corners under different structure configurations, and filling time are of particular interest. In example 1, shown in Fig.11, a tube of adhesive (density: 1.11E-6 Kg/mm^3; viscosity: 3.92E-5 GPa*ms; surface tension: 4.5E-8 KN/mm, contact angle: 0.698 radians) is being injected into an edge formed by two rigid plates with a gap of 0.2mm. The tube opening is being simplified and resulting in a close to half-round shape (free-surface side) of the formed bead. One could imagine the free surface of the formed bead would be flatter if the opening is tapered. In example 2, shown in Fig. 12a, in a similar setup as in Fig.11a, except a rigid plate is added in a 45° forward compound angle towards the formed adhesive bead, following the tube movement in a distance of 13mm behind. At the end of the simulation, squeezed out, excess adhesives are visible on the top edges of the top and bottom plates. Essentially, the optimal amount of adhesive, in terms of the tube diameter and the injection speed, can be optimized to result in less or no adhesive application in areas other than in the gap. In addition, because of the added plate wiping action, the fill depth (0.99mm) in the gap (Fig.12f) is triple the size (0.33mm) of that in example 1, Fig.11f, potentially making the bonding much stronger. The fill depth can also be used as an optimization objective.

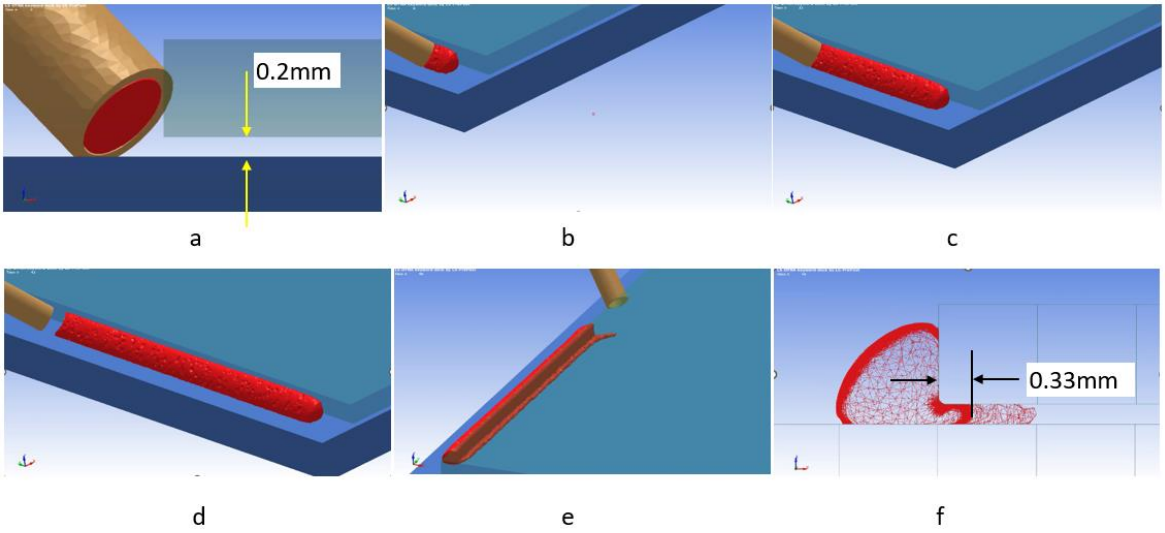

Fig.11: Injected adhesive application example I.

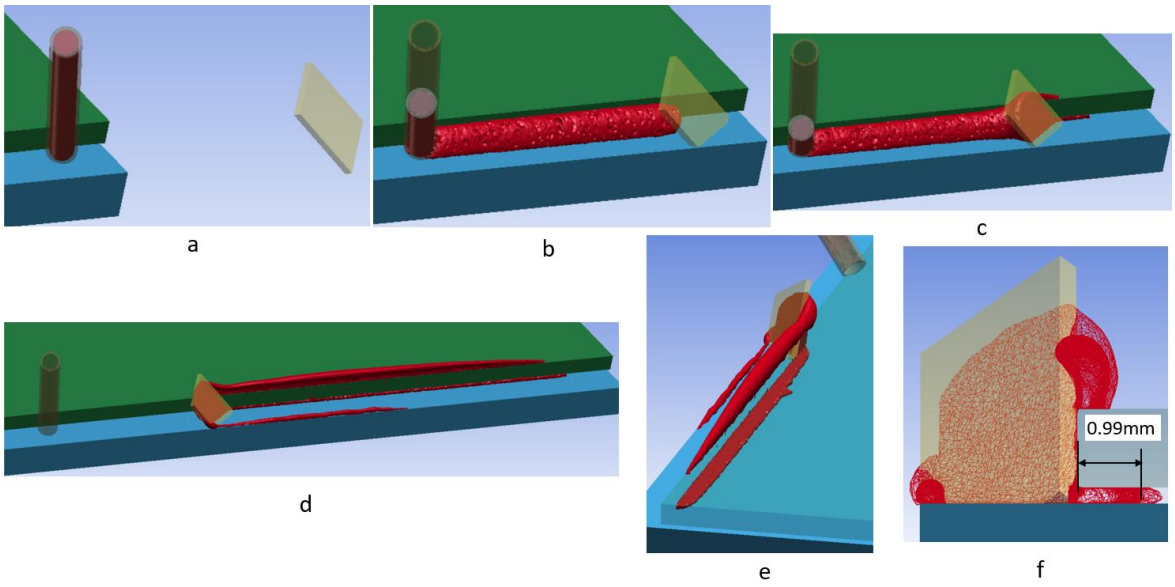

Fig.12: Injected adhesive application example II.

Metal hemming is an important part of the vehicle assembly process in the automotive and appliance etc. industries, where adhesives are frequently used. In the automotive industry, all closure panels, such as front and rear door outer/inner panels, hood outer/inner panels, and decklid outer/inner panels, are typically hemmed together around the perimeter. Here, we explore how adhesive, typically applied between outer and inner panels before hemming, behaves in the process. In Figs.13a (side view), and 13b (isometric view), an example hemming model in an inclined angle is set up, consisting of pre-hem steel (rigid body), which runs parallel to the hem surface, followed by a final-hem steel (rigid body) coming down in the direction perpendicular to the hem surface. This setup corresponds to the hem condition of a hood inner/outer assembly, where hem surfaces are often at an angle to the horizontal plane. Typical parts (Fig.13a) involved in a hemming operation often include deformable outer and inner panels, clamping devices (rigid bodies) for both the outer and inner panels, anti-flutter rubber (deformable), and hem bed (rigid body). The outer, with its periphery flanges typically already flanged to a $90°$ angle to the hem surface in a previous stamping operation, is placed and clamped on the hem bed; the inner panel goes on top of the outer and clamped down against the outer with some anti-flutter rubbers in between. Just prior to placing the inner, adhesive (density: 1.22E-6 Kg/mm^3; viscosity: 1.9E-5 GPa*ms; surface tension: 2.0E-8 KN/mm, contact angle: 0.698 radians) is applied on the outer inboard of the flanged area (Fig.13a). The small insert in the figure shows the gravity effect on the adhesive, which initially modeled as a long, square block (Fig.13b). Fig.13c shows the adhesive bead after the inner is clamped down. Fig.13d shows the adhesive shape after pre-hemming, and Figs.13e and 13f show the final hemmed configuration in two different views. Given the manufacturing process parameters, these types of simulation (digital DOEs) can be conducted to ascertain the bond strength before the start of production or even before the prototype build, to develop countermeasures to address issues such as the optimal amount and the placement of adhesives, the pressures applied to various deformable, the continuity of the adhesive spread and coverage, including dry-spot/squeeze-out zones, insufficient filling, etc. which could lead to corrosion.

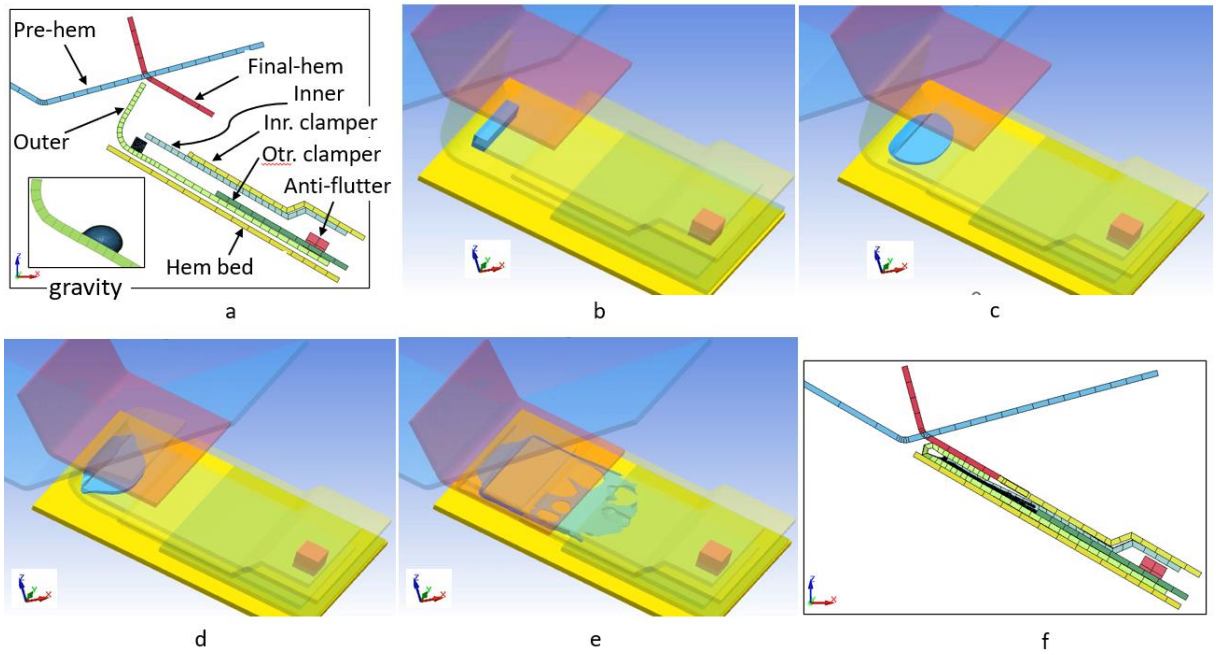

Fig.13: An example of adhesive application in an inclined hemming situation.

In the semiconductor industry, a flip chip package is made by flipping an Integrated Circuit (IC) upside down and its solder bumps are directly bonded to the corresponding contact pads on the substrate or Printed Circuit Board (PCB). Underfilling (Fig.14) is the process of applying a non-conductive adhesive (for example, epoxy), between a flip-chip die and a substrate. Also shown in Fig.14 are different components involved in the underfilling process. Underfilling materials distribute stresses among solder joints, improve solder fatigue resistance, and protect the die from moisture and other environmental conditions. Underfill materials enhance the overall performance of the flip chip and chip-scale packages. The dimensions involved in the flip-chip underfilling are usually very tiny, often in the order of micrometers. In Fig.15, a small underfilling example involving two columns of epoxies (density: 1.11E-6 Kg/mm^3; viscosity: 1.18E-6 GPa*ms; surface tension: 5.1e-8 KN/mm, contact angle: 0.698 radians) placed on two sides, to underfill a gap of 0.5mm (other dimensions also shown in the figure) consisted of solder balls and other chips. At t=650ms, the two columns of epoxies collapsed under

gravity onto the top of the flip-chip and started to fill the gap. At t=1700ms, the epoxies on top of the flip-chip started to be drawn more into the gap, and at t=5000ms, it completely filled the gap, wrapped around the solder balls and other spaces formed by other chips, and no epoxy left on top of the flip-chip.

In Fig.16, an underfilling process of 100 solder balls is shown, with the same epoxy properties stated above. In this case we assume the epoxies are positioned at all four edges, and underfill towards the center. No air trap is considered. The ISPG/structure coupling performed very well and fluid boundaries aligned perfectly with solder balls geometries. The simulation took about 20 hours on one core in MPP mode.

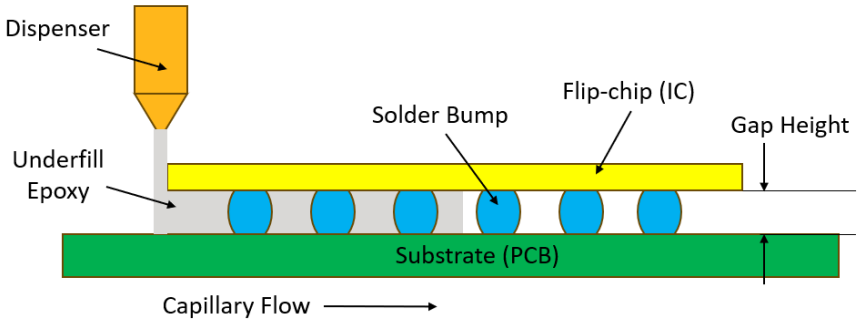

Fig.14: The underfilling process in a flip-chip.

In Fig.17, the solder ball numbers was increased to 528, with the same ball size and spacing, and epoxy properties as before. The intial number of nodes on the ISPG fluid is 13770, reaching 127040 nodes in the end. The progression of an underfillling process is shown and the fluid boundaries aligned perfectly with solder balls geometries.

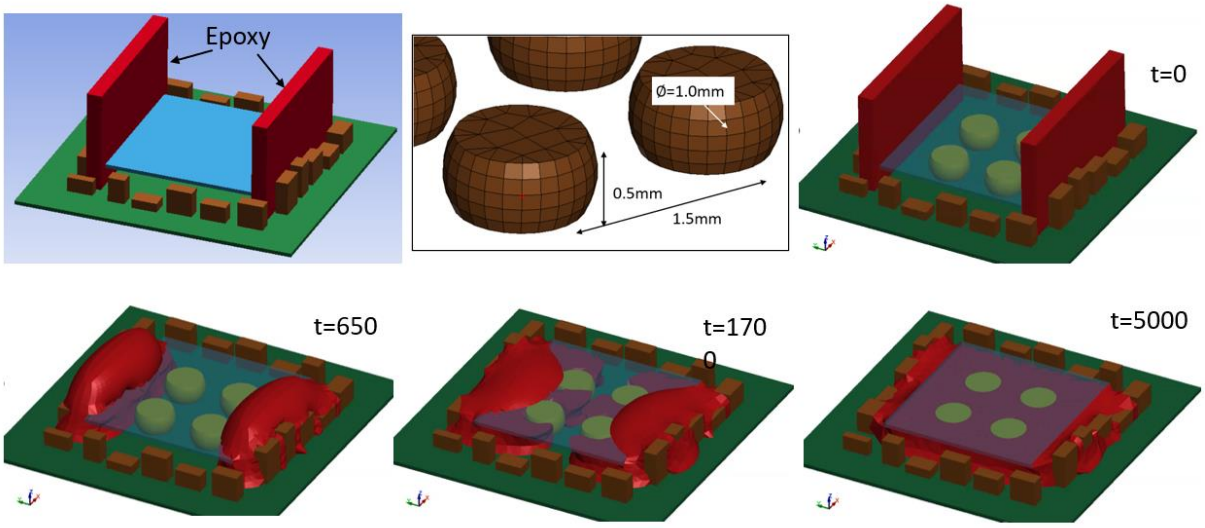

Fig.15: A small underfilling example in a flip-chip (time unit: ms).

In Fig.18, we attempt to correlate the ISPG simulation with experimental measurement [5] in an underfilling process simulation. The Newtonian model is used for the adhesive (density=1.103E-3 g/mm^3; viscosity: 1.118E-3 MPa*ms; surface tension: 5.1e-5 N/mm). The ball size, spacing, and gap height are shown in Fig.18a. The initial number of nodes on the ISPG fluid is 23332, reaching 155849 in the end. The volume of the ISPG remains near constant (2.50067 mm^3 final vs. 2.50063 mm^3 initial). The experimental photo of the underfilling at t=10s is shown in Fig.18b, while the ISPG simulation at the same time is shown in Fig.18c right. The last filled state available from the experiment is shown in Fig.18d, and the corresponding one from the simulation is shown in Fig.18e. A comparison between the experiment and simulation indicates the fill wavefront shapes was captured very well, although the fill time needs to be improved. We continue to explore various physics that affect the fluid front shape and fill time, etc., which includes but is not limited to initial ISPG mesh size, viscosity, surface tension, Navier slip length for friction, contact angle for adhesion force, etc. Generally, the computational cost increases with more solder balls and smaller size of solder balls, as ISPG mesh will increase.

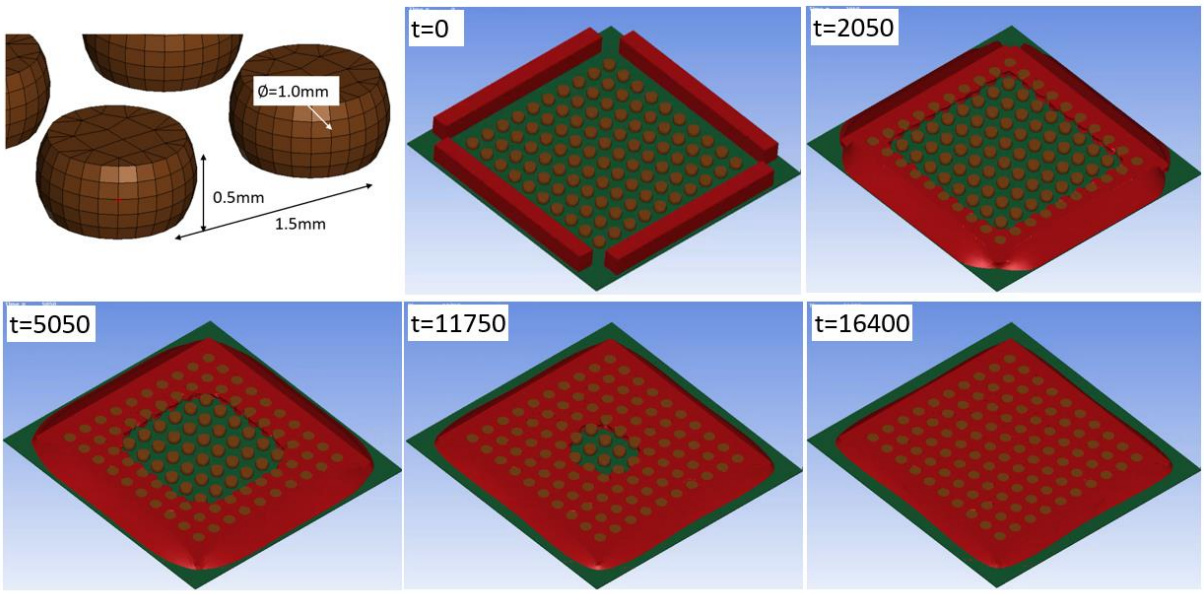

Fig.16: Underfilling of 100 solder balls of a flip-chip Ball Grid Array (BGA) (time unit: ms).

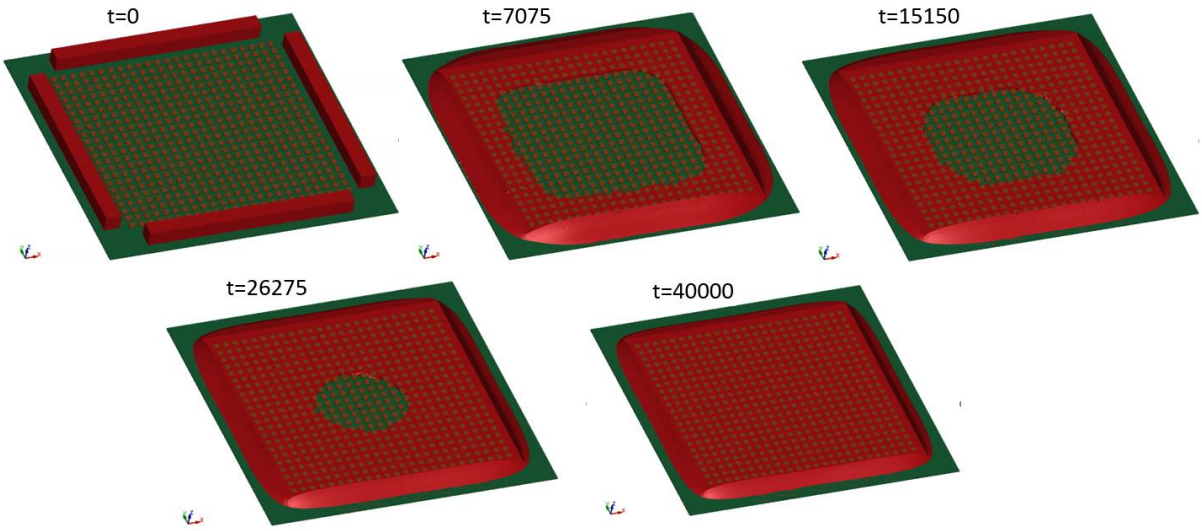

Fig.17: Underfilling of 528 solder balls of a flip-chip BGA (time unit: ms).

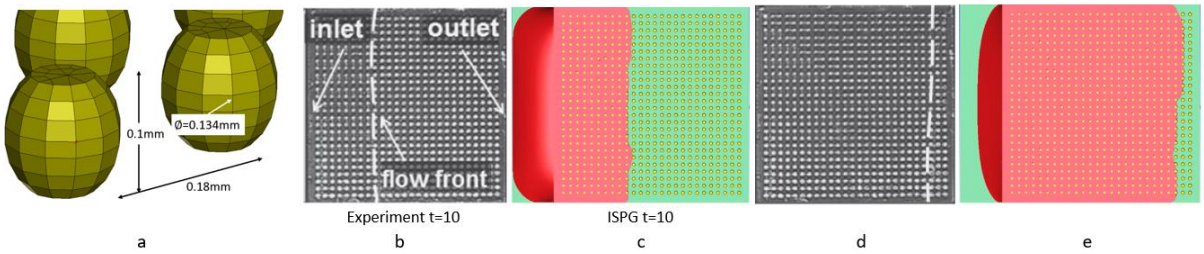

Fig.18: Underfilling of 676 solder balls of a flip-chip BGA (time unit: s).

8.4 Solder Paste

In the semiconductor industry, solder paste is applied to a printed circuit board (PCB) using a dispenser or stencil printing machine. Solder paste is a mixture of metal solder powder and flux that is required to successfully solder together a flip-chip and a substrate PCB. The correct amount of paste deposit needs to be applied to prevent soldering defects later on. The stencil is then removed to leave the solder paste in a column shape, so it stands alone on the PCB for soldering. The most common method of applying

solder paste to a PCB is through squeegee blade printing. The squeegees are tools used to apply pressure and move solder paste across a stencil, filling the gap in the process, and onto the PCB. They are usually made from flexible materials such as thin metal or polyurethane. Figs.19a and19b illustrate the basic components and dimensions involved in the simulation. The initial TETRA mesh edge length for the ISPG paste is 0.2x0.2x0.2mm. Note that the mesh size needs to be smaller than the stencil aperture diameter of 0.86mm. The Carreau model is used for the adhesive (density=5.0E-3 g/mm^3, visc0=6.0E+4 MPa*ms, vismax=1.0E-2 MPa*ms, lamda=1.0E6 ms, n=-0.04). Fig.19c shows the initial state of the simulation on a side view. In Fig.19d, the squeegee is pressed down (v=0.03mm/ms) and bent, deforms the solder paste, and pressed against the stencil. The bent squeegee is then moved (v=0.03mm/ms) along the stencil surface for a distance of 15.5mm (Fig.19e), filling the stencil aperture with the paste along the way. Figs.19f (side view) and 19g (isometric view) show the final state of the paste printing, which indicate most of the solder apertures are fully filled. In Fig.19h, the stencil is lifted up (v=0.003mm/ms), leaving the printed solder paste standing on the PCB, ready for soldering. In practice, variables such as squeegee pressure, velocity, and stencil removal speed, in addition to the paste properties, are some of the factors that affect the fill quality and paste residuals that remain on the stencil aperture after removal. Optimization involving these variables will ensure better solder paste configurations going into the soldering process.

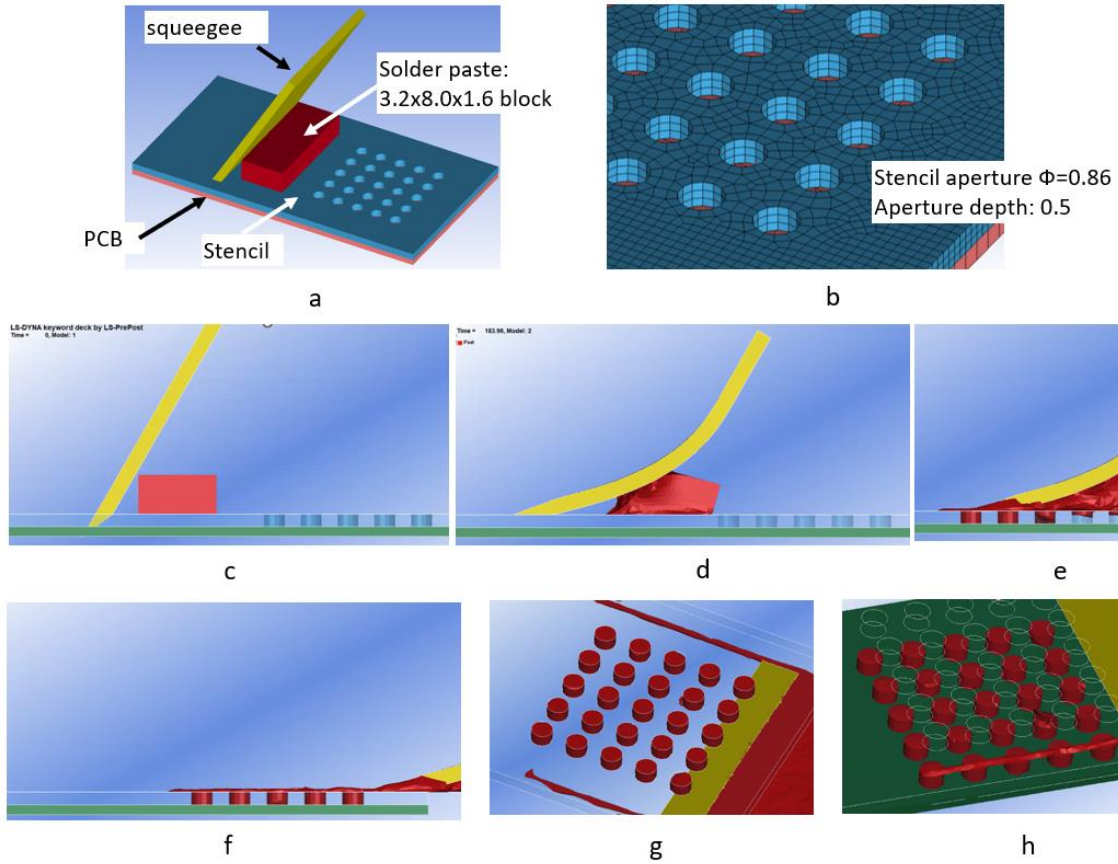

Fig.19: Solder paste printing and stencil removal (units: mm, ms).

9 Summary/Conclusion

The ISPG method benefits from the highly efficient Lagrangian adaptive remeshing, where the particles move with material flow. Therefore, it does not require uniform, tiny elements to capture structural details, especially for these tool areas with sharp corners and edges. Because of the various techniques used, the fluid edge can capture and align exactly with structure boundaries. The implicit method is very automated, requires minimal user inputs, and is therefore easy to use. The final resulting Lagrangian mesh from an ISPG simulation can also be used for subsequent analysis/simulation. These advantages are the most appealing to potential users, especially those who traditionally specialize in the solid mechanics area.

The ISPG method is currently limited to being run with one core in MPP mode for applications other than solder reflow, which limits the model size. For large models, such as underfilling for 600 solder

balls, computational time could be prohibitive. In addition, the ISPG fluid interface with deformable structures will need a strong coupling to make the simulation stable. Multiphase, including air, would also be vital in many applications. In the thermal coupling area, a two-way fluid/structure interface is under development. Solidification and porosity are also expected. We look forward to these limitations being lifted soon so the ISPG method can be expanded into even wider application areas.

10 Literature

[1] X. Pan, C.T. Wu, W, Wu, “Incompressible Smoothed Particle Galerkin (ISPG) Method for an efficient Simulation of Surface Tension and Wall Adhesion Effects in the 3D Reflow Soldering Process”, 16th International LS-DYNA Users Conference, June 10-11, 2020.
[2] A. Kumar, V. Pawar, “Die Attach Process using Adaptive ISPG in LS-DYNA”, 14th European LS-DYNA Conference 2023, Baden-Baden, Germany.
[3] LS-DYNA/ISPG Keyword and Material Model Manuals.
[4] X. Pan, C. T. Wu and W. Hu, “A semi-implicit stabilized particle Galerkin method for incompressible free surface simulations”, Int. J. Numer. Methods Eng., in press, doi: 10.1002/nme.6396, 2020.
[5] S. H. Lee, H. J. Lee, J. M. Kim and Y. E. Shin, “Dynamic Filling Characteristics of a Capillary Driven Underfill Process in Flip-Chip Packaging”, Materials Transactions, Vol. 52, No. 10 (2011) pp. 1998 to 2003.